Flexible Phase-Domain Synchronous-Machine Model with Internal Fault for Protection Relay Testing and related Real-Time Implementation Issues

P. Le-Huy[1], C. Larose[1], F. Giguère[2]

[1] Institut de recherche d'Hydro-Québec; [2] Hydro-Québec Production

Abstract—**This paper presents a real-time phase-domain synchronous machine model for generator protection relay testing and its real-time implementation. The model allows full protection scheme validation including split-phase differential and stator-ground fault protections. Space harmonics are considered through the use of modified winding function theory, which is used to represent arbitrary winding distributions and internal asymmetries, such as internal faults. The model and its theoretical basis are briefly presented; the real-time implementation, its results and the issues encountered in relation to the model computation complexity are discussed. Finally, the real-time hardware-in-the-loop (HIL) testing of a generator protection relay is detailed.**

Keywords: **Internal fault, parallel-connected windings, phase-domain modeling, protection relay, real-time simulation, space harmonics, synchronous machine, winding function.**

I. INTRODUCTION

SYNCHRONOUS alternators are the heart of power generating facilities and, as such, are protected and monitored by sophisticated devices. In order to safeguard the generators, protection relays typically monitor the alternator's terminal and neutral point voltages and several currents (in and out of each phase, neutral, field, etc.). With all this information, the relays are able to detect abnormal behaviors, such as internal faults, and cease operations to avoid or limit damage to the generator.

Before approving and commissioning generator protection relays, extensive testing is required, either as laboratory (or field) experimental testing or real-time hardware-in-the-loop (HIL) simulations, to validate protection schemes and determine appropriate settings. The first approach is time-consuming and costly while the latter is limited by the simulation models' abilities to represent adequately the synchronous-machine behavior with all its subtleties. On the other hand, real-time simulation allows the evaluation of the tested device's impact on the power grid and the identification of adverse interactions with existing equipments and controls.

The scientific literature presents several models of

synchronous machine that have been implemented for HIL simulations. A large portion of these models use the two-reaction theory which yields a dq0 representation of the machine [1]. Quite elegant and computationally efficient, this modeling shines in network studies or other situations where only the general behavior of the synchronous machine is required since major assumptions are made concerning the physical construction of the machine. For protection relay testing, where protection scheme rely on subtle phenomena to evaluate the machine state, a more complex representation is needed.

The phase-domain (PD) representation is able to overcome the shortcomings of the dq0 modeling by taking into account machine constructions realities such as parallel phase windings, arbitrary winding distributions and internal asymmetries. Several implementations have been presented for internal fault modeling, each with its own flavor (real-time or not, interfaced or embedded, current or voltage injections, etc.) [2]-[7]. While being very interesting, these models, as presented, are limited to single windings per phase or assume concentrated or sinusoidal-distributed windings, which is not representative of a majority of synchronous generators and limits the types of internal fault that can be portrayed. In fact, high power synchronous machine have several parallel-connected windings to form each phase, typically between two for high-rotation speed turbo-generators and six for low-speed hydraulic generators.

As for internal faults, the models mentioned consider only whole phase faults. In light of the parallel phase windings in real machines, the probabilities of a whole phase being shorted to ground, which implies multiple shorts occurring at exactly the same time on several windings spatially distributed around the machine stator, are rather slim and such situations are rather unrealistic.

The real-time implementation presented in this paper is an improved version of X. Tu's model [6]-[7] that supports parallel phase windings with arbitrary distributions and internal asymmetries, neutral impedance as well as internal stator-stator and stator-ground faults. Improvements include enhanced mathematical stability, refined real-time capabilities and full integration into Hypersim, a digital real-time simulator developed and used at Hydro-Québec's Research Institute [14]. Modified winding function theory [7] is used to calculate the inductances of the machine. This approach requires the machine's winding diagram or the sequential ordering of the winding conductors in addition to the usual standard electrical parameters. While it requires more data than other models, this technique allows arbitrary winding distributions and nonuniform air-gaps which translate into the presence of space harmonics in the machine's signals.

The rest of the paper is divided in four parts: Section II describes the simulation model while Section III discusses the real-time implementation and performances; Section IV presents a full protection scheme HIL testing of an Areva MiCOM P343 protection relay and, finally, concluding remarks are stated in Section V.

II. PHASE-DOMAIN SYNCHRONOUS-MACHINE MODELING

The present model keeps the fixed-reference frame for all stator windings (up to six per phase) but uses a d-q representation of the rotor [8] as seen in Fig. 1. Round-pole machines make use of all rotor windings (field, d damper and two dampers on the q axis) while only one q damper winding is necessary for salient-pole machines.

The voltage equations are expressed as

$$v_{abcs} = R_s i_{abcs} + s \lambda_{abcs}$$
$$v_{qdr} = R_r i_{qdr} + s \lambda_{qdr} \tag{1}$$

where s subscript variables refer to the phase-domain stator windings and the r subscripts to the d-q rotor elements. The size of the stator terms is equal to the total number of stator windings (to reduce the display size of the following formulas, a machine with single winding per phase is assumed). The flux linkage (λ) equation can be written as follows with stator-referenced rotor terms noted with a prime mark.

$$\begin{bmatrix} \lambda_{abcs} \\ \lambda'_{qdr} \end{bmatrix} = \begin{bmatrix} L_s(\theta_r) & L'_{sr}(\theta_r) \\ \frac{2}{3}(L'_{sr}(\theta_r))^T & L'_r \end{bmatrix} \begin{bmatrix} i_{abcs} \\ i'_{qdr} \end{bmatrix} \tag{2}$$

Using a non-uniform air-gap approximation, which yields a constant inductance L_A and a sinusoidal term, L_B, with twice the electrical rotor angular velocity, the stator inductance matrix L_s takes the following form:

$$L_s = \begin{bmatrix} L_{ls} + L_A - L_B\cos(A) & -L_A/2 - L_B\cos(B) & -L_A/2 - L_B\cos(C) \\ -L_A/2 - L_B\cos(B) & L_{ls} + L_A - L_B\cos(C) & -L_A/2 - L_B\cos(A) \\ -L_A/2 - L_B\cos(C) & -L_A/2 - L_B\cos(A) & L_{ls} + L_A - L_{B\cos}(B) \end{bmatrix} \tag{3}$$

L_{ls} is the leakage inductance and A, B and C equal to $2\theta_r$, $2\theta_r - 2\pi/3$ and $2\theta_r + 2\pi/3$ respectively.

The stator-rotor and rotor inductance matrices are defined in (4) and (5) where L_{md} and L_{mq} are the d- and q-axis magnetizing inductances and L'_{lfd}, L'_{lkd}, L'_{lkq1} and L'_{lkq2} the stator-referenced leakage inductance of the field, the d- and q-axis damper windings respectively.

$$L'_{sr} = \begin{bmatrix} L_{mq}\cos(\theta_r) & ... & L_{md}\sin(\theta_r) & ... \\ L_{mq}\cos(\theta_r - 2\pi/3) & ... & L_{md}\sin(\theta_r - 2\pi/3) & ... \\ L_{mq}\cos(\theta_r + 2\pi/3) & ... & L_{md}\sin(\theta_r + 2\pi/3) & ... \end{bmatrix} \tag{4}$$

$$L'_r = \begin{bmatrix} L'_{lkq1} + L_{mq} & L_{mq} & 0 & 0 \\ L_{mq} & L'_{lkq2} + L_{mq} & 0 & 0 \\ 0 & 0 & L'_{lfd} + L_{md} & L_{md} \\ 0 & 0 & L_{md} & L'_{lkd} + L_{md} \end{bmatrix} \tag{5}$$

Equations (3) and (4) assume sinusoidal stator windings for simplicity's sake; arbitrary winding distributions alter slightly

the form of the stator related terms as presented later in this section.

If all these winding inductances and related resistances, (usually referred to as "fundamental" parameters) are not available for a given machine, they can be deduced from the more easily procurable "standard" parameters (X_d, X_d', X_d'', etc.) by using available conversion methods [9]-[10].
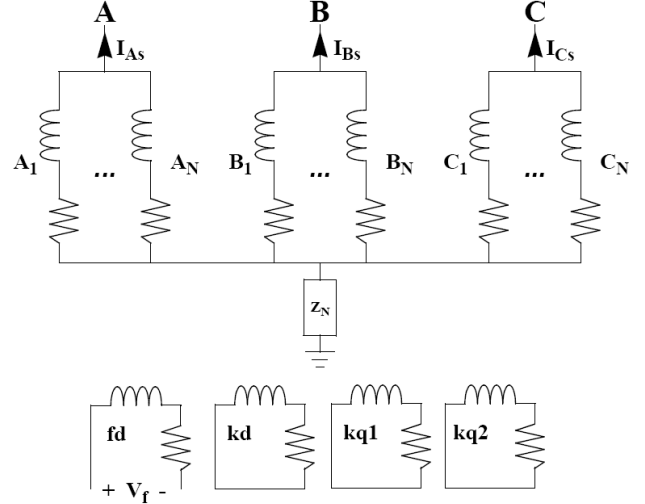
Fig. 1. Diagram of N parallel-connected winding circuits per phase with neutral impedance (upper) and d-q rotor representation with field and three damper windings (lower).

Before describing the inductance calculations, a brief overview of winding function theory is given.

A. Winding Functions

The subtleties of the physical construction of synchronous machines used in power generating facilities are more than often neglected in models used for transient and stability simulations. Winding function theory is widely used to incorporate details of the machine construction into the inductance analytical calculations [5]-[7][11][12]. This representation of the windings is in a fact a simplified image of the magnetomotive force as a function of the spatial distribution around the stator structure of the windings' coils. In the present model, each stator winding is represented by its winding function in order to establish the self and mutual inductances. The winding functions are easily constructed from the machine characteristics: number of poles, stator slots, conductors per slots and the winding order of the machine, i.e. the sequence of slots occupied by specific coils. As one can observe from Fig. 2, winding functions allow a more realistic representation of the windings, which will translate as harmonics in the machine's currents and voltages.

B. Inductance calculations

Once the winding functions for all windings are established, they are used in the following expression to compute the self and mutual stator inductances:

$$L_{yx} = L_{xy} = K_0 A_{xy} - K_2 B_{xy} \tag{6}$$

$$A_{xy} = \langle n_x n_y \rangle - \langle n_x \rangle \langle n_y \rangle$$
$$B_{xy} = \langle n_x n_y \cos(2p(\phi - \theta_r)) \rangle - \langle n_x \rangle \langle n_y \cos(2p(\phi - \theta_r)) \rangle \tag{7}$$
$$- \langle n_y \rangle \langle n_x \cos(2p(\phi - \theta_r)) \rangle$$

where $\langle X \rangle$ is the average value of X on a 2π interval, n_x the

winding function of x, p the number of pairs of poles, θ_r the electrical rotor angle, ϕ the inspection angle around the stator and K_x are geometrical coefficients. Since winding functions are solely a function of ϕ, (7) can be reduced to this simplified form:

$$L_{yx}(\theta_r) = L_{xy}(\theta_r) = L_{xy0} + L_{xy1}\cos(2p\theta_r) + L_{xy2}\sin(2p\theta_r) \quad (8)$$

It is of interest to note the similarity between the simplified form and the inductances expressions in (2). For perfectly sinusoidal winding distributions with ideal phase balance, all mutuals have the same continuous and alternate amplitude values and perfect spatial distribution ($2\pi/3$ phase spacing). These analytically convenient characteristics allow the passage to dq0 representation and in the process subtleties of the machine behavior are lost, which is unacceptable for the present application. Consequently, it is necessary to take into account the differences between self and mutual inductance in all the machine's windings.
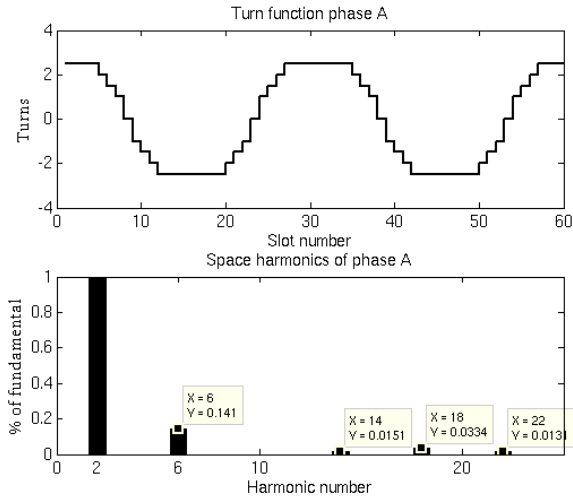
Fig. 2. Winding function example of twin parallel windings, four poles, 60-slot alternator and its related space harmonics. The fundamental space harmonic corresponds to the number of pairs of poles, two in this case. Higher harmonics with considerable amplitude are also present.

K_0 and K_2 are geometric coefficients that link the winding functions and the measured magnetizing inductances of the machine. They are established by first computing (6) with unity coefficients for L_{AA} and L_{AB}. Then, using the terms in the simplified form, the geometrical constants are obtained as shown in (9). All the stator inductances are then computed.

$$K_0 = \frac{(L_{md} + L_{mq})}{2(L_{AA0} - L_{AB0})} \quad K_2 = \frac{(L_{md} - L_{mq})}{\sqrt{L_{AA1}{}^2 + L_{AA2}{}^2} + 2\sqrt{L_{AB1}{}^2 + L_{AB2}{}^2}} \quad (9)$$

The approach is similar for stator-rotor mutual inductances, again with two geometrical constants.

$$K_{r1} = -\frac{L_{md}}{\int_0^{2\pi} n_A \cos(p\phi)\,d\phi} \quad K_{r2} = \frac{L_{mq}}{\int_0^{2\pi} n_A \cos(p\phi)\,d\phi} \quad (10)$$

$$L'_{xfd} = L'_{xkd} = K_{r1}\langle n_x \sin(p(\phi-\theta))\rangle$$
$$L'_{xkq1} = L'_{xkq2} = K_{r2}\langle n_x \cos(p(\phi-\theta))\rangle \quad (11)$$

C. Internal Faults

Winding function theory is well suited to represent internal faults since these can be regarded as asymmetries in the winding distribution of the machine. The present model treats faulty windings as several normal windings, with lesser coils, connected to ground or to another phase winding in the case of stator-ground or stator-stator fault respectively as seen in Fig. 3. The winding functions of the sub-windings are computed and used to obtain the related self and mutual inductances. Additional equations are then inserted in (2).
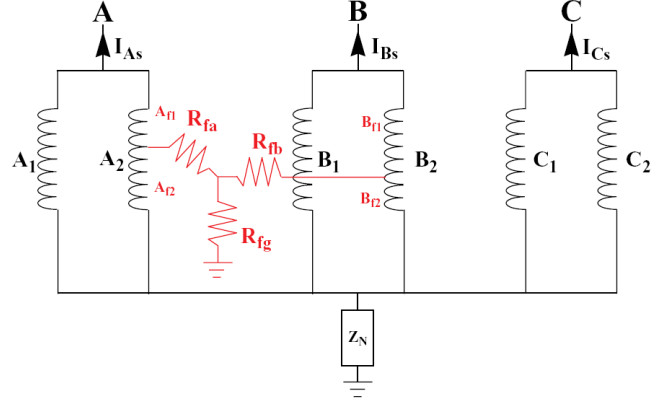
Fig. 3. Representation of an internal fault between winding A_2 and B_2 inside a twin parallel-connected winding machine. Each faulty winding is divided into two and connected through fault resistors. The type of the fault, stator-stator or stator-ground, is determined by the value of the different resistors.

The proposed model supports eight types of stator internal faults, namely:
- Single winding-ground;
- Shorted turns;
- Winding-winding (single, 2 and 3 phases);
- Winding-winding-ground (single, 2 and 3 phases).

III. REAL-TIME IMPLEMENTATION

The digital implementation of the model used (1) as the starting point to which was added the neutral and fault impedance matrix:

$$v(t) = (R + R_g + R_f)i(t) + s(L(t) + L_g + L_f)i(t) \quad (12)$$

where the voltage and current vectors take the following form for a N parallel-connected round-pole machine with winding A_2 faulted.

$$v = \begin{bmatrix} v_{A1}v_{Af1}v_{Af2}...v_{AN} & v_{B1}...v_{BN} & v_{C1}...v_{CN} & v_{fd}' & 0 & 0 & 0 \end{bmatrix}$$
$$i = \begin{bmatrix} i_{A1}i_{Af1}i_{Af2}...i_{AN} & i_{B1}...i_{BN} & i_{C1}...i_{CN} & i_{fd}' & i_{kd}' & i_{kq1}' & i_{kq2}' \end{bmatrix} \quad (13)$$

R is a diagonal matrix containing the winding resistances, L the rotor position dependent inductance block matrix defined in (2), g and f subscript matrices are filled with the ground and fault elements respectively. Here, one must remember that prime-marked variables are referenced to the stator side. Rearranging the equation and applying the trapezoidal discretization yields the recurrent equation below.

$$i_n = \left(X_n + \frac{\omega_b t_s}{2}R_T\right)^{-1}\left[\left(X_{n-1} - \frac{\omega_b t_s}{2}R_T\right)i_{n-1} + \frac{\omega_b t_s}{2}(v_n + v_{n-1})\right] \quad (14)$$

Variables with n and $n-1$ subscripts refer to the current and previous time step respectively, X contains the machine and ground inductances while R_T is the total resistance matrix, ω_b is

the nominal angular speed and t_s the time step length in seconds.

The present form was preferred over the approach taken in [7] since it lessens the already important computation burden. Furthermore, the discretization method used, as described in [13], has stability issues and adds a striking amount of computation work, that cannot be justified by the higher order accuracy for real-time performances.

A. Model Particularities

Porting the proposed model to real-time performances was challenging due to the time-varying inductance matrices and the number of highly-coupled differential equations to solve.

The phase-domain representation imposes that at every time step all the inductances be reevaluated for the current rotor position. This task can appear trivial but the high number of inductances to evaluate and the computation cost of trigonometric functions make it not so inconsequential. And thus, the simplified form used to evaluate the inductances presented in (8) was expressed as a weighted sine and cosine contribution instead of a single weighted sinusoidal function with a phase offset. In this manner, two trigonometric functions are executed to evaluate the $N(N+1)/2$ different terms in L_s, that would have otherwise required the same amount of trigonometric function calls.

Once the new inductance matrix is obtained, an inversion is required, as seen on the right-hand side of (14). Since the actual invert is not required, a LDL^T Cholesky factorization followed by forward/backward substitutions is an efficient way to obtain the machine's currents.

A possible work-around would be to precalculate the inverse for a certain number of rotor positions and access these values at runtime. Interpolation, typically linear, is then used to get the inverse corresponding to the exact rotor position. As discussed in [7] and [13], over 250 precalculated matrices are required for adequate simulation quality and the authors settled for 500 for their implementation. However, it was observed that, even with that resolution, after a few seconds of simulation, the tabulated method resulted in a little offset in the machine's currents, particularly the field current. Higher resolution is mandatory in this case. These observations exacerbate the already important memory requirements of this approach (e.g. 720 25x25 matrices of double precision value equal approximately 3.51 MB) and execution performance would be slightly degraded due to higher cache level and/or RAM access. Nonetheless, if memory requirements are of no concern and numerous high-level cache access of no consequence, precalculation yields the fastest execution time.

B. Internal Fault Modeling

As illustrated in Fig. 3, internal faults are represented by splitting faulty windings in sub-windings with fewer coils and fault resistances are added to the internal circuit. A two resistor approach was used to keep the same matrix dimensions throughout the entire simulation. The internal fault is activated by going from a really high value (> 1 MΩ) to a small one (< 1 mΩ).

Under normal operating conditions, parallel-connected windings carry the same current. Thus using a lumped-equivalent winding leads to an execution time reduction for healthy machines. This approach is interesting if internal faults are not mandatory. Otherwise, once the fault happens, all windings must be considered separately since they do not respond exactly in the same way to the internal asymmetry introduced by the fault. Switching back and forth between the full and the reduced equation set might be tricky depending upon the specific implementation and integration method. Furthermore, one must remember that in the end, it is the execution time of the faulty machine that dictates the usable time step threshold for real-time performances.

C. Results and performances

A 370 MVA, 13.8 kV, 48 salient poles machine with six parallel-connected windings per phase was used to evaluate the execution time of the presented model on a Sgi Altix 4700 computer sporting Intel's Itanium series 9000 processors.

Figure 4 illustrates simulation results for a single winding-to-ground fault at 45% of the winding. All parallel-connected winding currents are shown in addition to the neutral impedance's current. In steady state before the fault, each parallel winding carries a sixth of the total phase current. In this example, the phase current is approximately 91% of the nominal peak value or around 14.2 kA$_{rms}$ and thus each parallel winding carries around 15% of the whole phase nominal peak value, as shown in Fig. 4. As can be observed at 0.05 s, the fault is applied, resulting in disturbances in the phase A currents while phases B and C are less affected. It is important to notice that the parallel-connected windings of a specific phase do not carry the same current during an internal fault, since the relation of each individual winding to the faulty windings are not the same. This phenomenon can be exploited for a split-phase differential protection scheme. Such subtle cases are really challenging for models that do not consider parallel-connected windings.

The ground current presents the characteristic third harmonic component with an rms value of 0.92 A (the neutral point is grounded through a high-value RL impedance). Once the fault is applied, the ground current's peak value jumped by a factor of almost eight.

An example of shorted-turn fault simulation is given in Fig. 5. This type of fault is difficult to detect due to the very limited impact on the monitored machine signals, as seen on the terminal currents, and often leads to critical damage to the generator due to excessive currents experienced by the shorted turns (Af2 carries almost four times its nominal current).

The execution time of the presented model falls between 33 and 39 μs for all the supported fault types. This also includes interprocessor communication time since the internal-fault machine model is an independent simulation task, which means that the model imposes no limits on the size of the simulated power network to which is it attached.

Once real-time performance was achieved, a generator protection relay was connected to the simulator and the model was put to the test.

IV. Protection Relay Testing

For generator protection, numerous protection devices are implemented by the relay, as shown in Table I. It is interesting to note that the presented model is able to provide realistic signals to test all the listed protection devices whereas a conventional dq0 model would be hard-pressed for differential

and stator-ground protection devices. Furthermore, the suggested model is one of the few that allows validation of split-phase differential protections (parallel-connected windings are split in two groups and the difference between the current flowing in each group serves to identify internal faults).
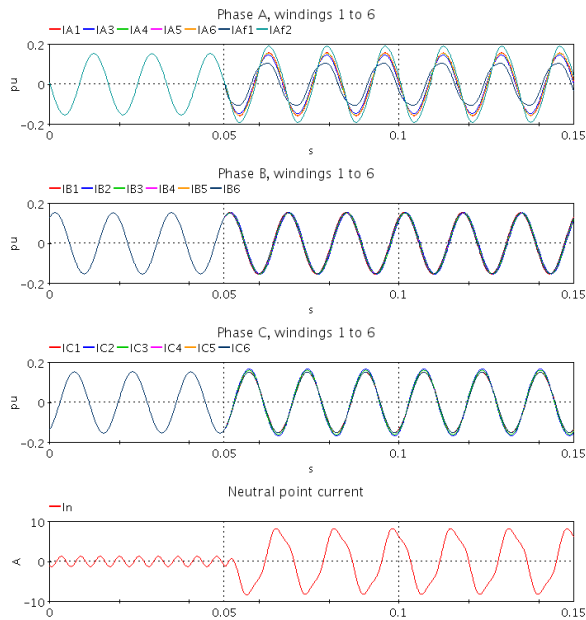
Fig. 4. Winding currents following a 45% stator-ground fault on winding A2 in a six parallel-connected winding generator (total steady state phase current of 0.92 pu divided equally among the six healthy parallel phase windings) and neutral point current exhibiting distinctive third harmonic content.
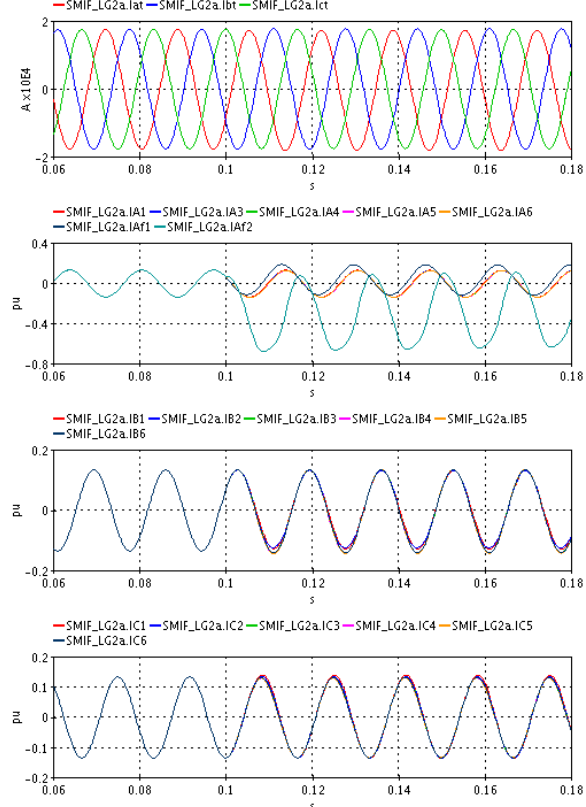
Fig. 5. Terminal (whole-phase) and winding currents following a 50-40% shorted-turn fault on winding A2 in a six parallel-connected winding generator.

A. Experimental setup

For the experimentation, the simplified schematic illustrated in Fig. 6 was implemented and simulated with Hypersim. Two generators connected to the network through a three-winding transformer are represented here since the modeled machine is used in such way in the field.

Alternator A1 is a generic machine and A2 is the winding function model with internal fault. Both machines are 370-MVA, 13.8-kV, 60-Hz and 48-salient-pole hydraulic alternators (the winding function model has six parallel-connected windings per phase). The machine standard parameters can be found in [13] but fundamental parameters were obtained using the conversion method described in [9]-[10].

TABLE I
USUAL PROTECTION DEVICE IN GENERATOR PROTECTION RELAY

Device	Description
21P/C	Phase Mho or Compensator distance
24	Volts-per-Hertz
25	Synchronism check
27	Undervoltage
32	Directional power
40	Loss-of-field
46	Negative sequence overcurrent
50P/G/N/Q	Overcurrent (Phase, Ground, Neutral, neg. seQ.)
51G/N/V/C	Time overcurrent (Ground, Neutral, Voltage restrained / Controlled)
59P/G/Q/N	Overvoltage (Phase, Ground, neg. seQ., Neutral)
60	Loss-of-potential
64G	100-percent stator-ground
78	Out-of-step
81O/U	Frequency (Over, Under)
87/N	Current Differential with terminal and neutral point current or with neutral impedance current (N)
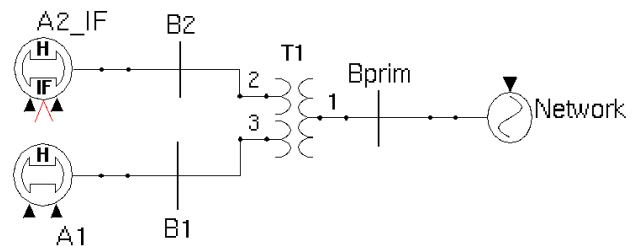
Fig. 6. Simplified schematic of the simulated network for protection relay testing.
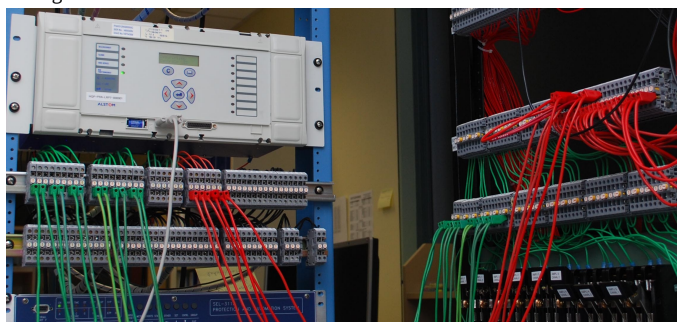
Fig. 7. Experimental setup for generator protection relay testing (the relay under test is an Areva MiCOM P343).

The relay under test is an Areva MiCOM P343 implementing most of the listed devices in Table I and more with the same settings and timing parameters as those in the field. The B2 bus bar voltages, terminal currents, neutral point currents and neutral point voltage are fed to the protection relay through current and voltage amplifiers connected to the digital simulator

as shown in Fig. 7. This signal conditioning is necessary since this specific relay expects a certain current and voltage level coming from the current or potential transformers.

B. Results

The real-time simulation was done with a 50-µs time step on a Sgi Altix with a single Itanium 2 processor. Several protection devices were tested but 95% and 100% stator-ground (64-1 and 64-2) as well as current differential (87) were tested more intensively. As expected, the field parameters were adequate to successfully detect internal faults of various types. Figure 8 illustrates comtrade recordings obtained from the P343 after a stator-stator fault. Protection relays are set to be extremely sensitive to complete-phase in and out current differentials and typically no delay device is implemented. This can be observed from the faultograph signals: as soon as the current differential is detected, approximately 0.6 cycles after the fault, protection device 87A is tripped simultaneously with the global generator isolation (S1 94C-2A-2B/A) signal.
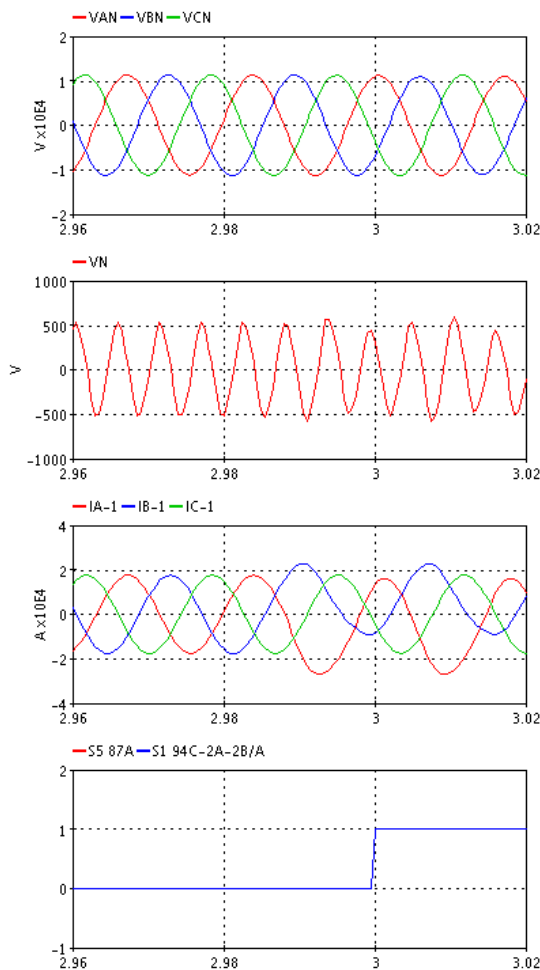
Fig. 8. Monitored signals extracted from the COMTRADE file generated after a stator-stator fault (A2 50% - B2 45%). Differential protection device was tripped (87A) which resulted in the simultaneous shutdown of the generator (94C).

V. Conclusions

A flexible phase-domain synchronous machine model and its real-time implementation were discussed and its usage demonstrated for generator protection relay testing. The first part of the paper briefly explained the model and the inductance calculations based on winding function theory. This method allows representation of space harmonics due to the spatial distribution of the windings around the machine's stator. Thus, the simulated machine exhibits the signature of a specific stator construction instead of the almost "theoretical" sinusoidal distribution assumed in conventional machine models. Furthermore, the presented model considers parallel-connected windings, which permits more realistic stator faults unlike models that make the assumption of lumped-equivalent whole-phase windings. Fine tuning of relay settings also benefits from this feature since more subtle behavior disturbances can be represented. Real-time implementation issues are discussed in the second part of the paper. Challenges encountered and pitfalls of real-time modeling are described and the model's optimization since its previous incarnation is explained. The third part of the paper gave an example of generator protection relay testing. This model allows testing of all typical protection devices used for generator protection and, since all the parallel-connected winding currents are available, differential protection schemes are not limited to a complete phase. This last feature can be exploited for the development of more complex protection schemes.

VI. References

[1] P.H. Park, "Two reaction theory of synchronous machine," *AIEE Trans.*, vol. 48, pt. 1, pp. 716–730, Jul. 1929.

[2] D. Muthumuni, P.G. Mclaren, E. Dirks, and V. Pathirana, "A synchronous machine model to analyze internal faults," in *Conf. Rec. 2001 IEEE Ind. Appl. Conf.*, Chicago, IL, Sept. 30-Oct. 4, vol. 3, pp. 1595–1600.

[3] P.P. Reichmeider, C.A. Gross, D. Querrey, D. Novosel, and S. Salon, "Internal faults in synchronous machines part I: The machine model," I*EEE Trans. Ind. Electron.*, vol. 15, no. 4, pp. 376–379, Dec. 2000.

[4] S.D. Pekarek, O. Wasynczuk, and H.J. Hegner, "An efficient and accurate model for simulation and analysis of synchronous machine/converter systems," *IEEE Trans. Energy Convers.*, vol. 13, no. 1, pp. 42–48, Mar. 1998.

[5] A.B. Dehkordi, A.M. Gole, T.L. Maguire, and P. Neti, "A real-time model for testing stator-ground fault protection schemes of synchronous machines," *2009 Int. Conf. on Power Systems Transients IPST2009*, Kyoto, Japan, June 3-6, 2009.

[6] X. Tu, L.-A. Dessaint, M. El Kahel, and A. Barry, "A new model of synchronous machine internal faults based on winding distribution," *IEEE Trans. Ind. Electron.*, vol. 53, no. 6, pp. 1818–1828, Dec. 2006.

[7] X. Tu, L.-A. Dessaint, N. Fallati, and B. De Kelper, "Modeling and Real-Time Simulation of Internal Faults in Synchronous Generators With Parallel-Connected Windings," *IEEE Trans. Ind. Electron.*, vol. 54, no. 3, pp. 1400–1409, June 2007.

[8] P. C. Krause, O. Wasynczuck, and S. D. Sudhoff, *Analysis of Electric Machinery and Drive System*, 2nd ed., Pitscataway, NJ: IEEE Press, 2002, p. 191.

[9] L. Salvatore and M. Savino, "Exact relationships between parameters and test data for models of synchronous machines," *Electrical Machines and Power Systems*, vol.8, n.3, pp.169-184, June 1983.

[10] H.W. Dommel, *EMTP Theory Book*, 2nd. ed., Microtran Power System Analysis Corporation, Vancovuer, B.C., May 1992.

[11] I. Tabatabaei, J. Faiz, H. Lesani, and M. T. Nabavi-Razavi, "Modeling and Simulation of a Salient-Pole Synchronous Generator With Dynamic Eccentricity Using Modified Winding Function Theory," *IEEE Trans. Magnetics*, vol. 40, no. 3, pp. 1550–1555, May 2004.

[12] H.A. Toliyat, and N.A. Al-Nuaim, "Simulation and Detection of Dynamic Air-Gap Eccentricity in Salient-Pole Synchronous Machines," *IEEE Trans. Ind. App.*, vol. 35, no. 1, pp. 86–93, Jan. 1999.

[13] N. Fallati, "Implantation dans Hypersim d'un modèle de défauts internes dans la machine synchrone," M.Sc. Dissertation, Dept. Elec. Eng., ETS, Montréal, 2005.

[14] D. Van Que, J.C. Soumange, G. Sybille, G. Turmel, P. Giroux, G. Cloutier, S. Poulin, "Hypersim--an integrated real-time simulator for power networks and control systems," Proc. Int. Conf. Digital Power System Simulators, Vasteras, Sweden, May 1999.